Available online at www.sciencedirect.com
ScienceDirect
Journal of Nutritional Biochemistry 17 (2006) 811–820
Journal of Nutritional Biochemistry

RESEARCH ARTICLES

A type IV P-type ATPase affects insulin-mediated glucose uptake in adipose tissue and skeletal muscle in mice☆

Madhu S. Dhar[a,*], Joshua S. Yuan[b], Sarah B. Elliott[a], Carla Sommardahl[a]

[a]*Large Animal Clinical Sciences, College of Veterinary Medicine, University of Tennessee, Knoxville, TN 37996-4500, USA*
[b]*The UTIA Genomics Hub, University of Tennessee, Knoxville, TN 37996, USA*

Received 4 November 2005; received in revised form 27 December 2005; accepted 3 January 2006

Abstract

Mice carrying two *pink-eyed dilution* (*p*) locus heterozygous deletions represent a novel polygenic mouse model of type 2 diabetes associated with obesity. *Atp10c*, a putative aminophospholipid transporter on mouse chromosome 7, is a candidate for the phenotype. The phenotype is diet-induced. As a next logical step in the validation and characterization of the model, experiments to analyze metabolic abnormalities associated with these mice were carried out. Results demonstrate that mutants (inheriting the *p* deletion maternally) heterozygous for *Atp10c* are hyperinsulinemic, insulin-resistant and have an altered insulin-stimulated response in peripheral tissues. Adipose tissue and the skeletal muscle are the targets, and GLUT4-mediated glucose uptake is the specific metabolic pathway associated with *Atp10c* deletion. Insulin resistance primarily affects the adipose tissue and the skeletal muscle, and the effect in the liver is secondary. Gene expression profiling using microarray and real-time PCR show significant changes in the expression of four genes — *Vamp2, Dok1*, *Glut4* and *Mapk14* — involved in insulin signaling. The expression of *Atp10c* is also significantly altered in the adipose tissue and the soleus muscle. The most striking observation is the loss of *Atp10c* expression in the mutants, specifically in the soleus muscle, after eating the high-fat diet for 12 weeks. In conclusion, experiments suggest that the target genes and/or their cognate factors in conjunction with *Atp10c* presumably affect the normal translocation and sequestration of GLUT4 in both the target tissues.

Keywords: *Atp10c*; *Glut4*; Insulin signaling; Type 2 diabetes; Aminophospholipid translocase; Protein trafficking

1. Introduction

The incidence of type 2 diabetes (T2D) and obesity is increasing rapidly and reaching epidemic proportions. Insulin resistance is a key feature in both conditions and plays an important pathophysiological role [1–4]. Insulin resistance refers to the normal synthesis of the hormone, coupled with an altered response in the peripheral tissues. Insulin is the primary regulator of blood glucose concentration. Metabolic insulin signaling is dependent on protein–protein interaction and phosphorylation events. Glucose homeostasis is tightly controlled by a balance between glucose absorption from the intestine, production primarily by the liver, and uptake and metabolism by the skeletal muscle and fat. It is maintained by a fine interplay between the three target tissues — skeletal muscle, liver and adipose tissue. Defective glucose transport is a key rate-limiting step involved in the impaired glucose uptake in the peripheral tissues. Numerous studies show that the defects in insulin signaling pathways leading to GLUT4 translocation are important to the pathogenesis of insulin resistance. These defects might include changes in protein expression at the posttranslational level and/or alteration in gene expression at the posttranscriptional level. The question on how impaired glucose uptake and defective insulin signaling in the adipose tissue and the skeletal muscle contributes to whole body insulin resistance, however, is still unanswered [1–7]. Targeting insulin resistance has become an important new therapeutic goal in the treatment of T2D.

Human obesity, T2D, atherosclerosis and nonalcoholic fatty liver disease are influenced by genetic and environmental factors. Due to the complexities in the study of human obesity syndromes, animal models have been used

☆ This study was supported by the American Heart Association Beginning Grant-in-aid 0465188B (M.S. Dhar).
* Corresponding author. Tel.: +1 865 974 5703; fax: +1 865 974 5773.
E-mail address: mdhar@utk.edu (M.S. Dhar).

0955-2863/$ – see front matter © 2006 Elsevier Inc. All rights reserved.
doi:10.1016/j.jnutbio.2006.01.002

and the data is then translated into human homologs and phenotypes. Polygenic rodent models of obesity and T2D are thought to more closely mimic the presumed polygenic inheritance of these complex disorders in humans than do the single-gene models [8–10].

Using genetic mapping and phenotypic analyses, we have identified two distally extending heterozygous deletions, viz., $p^{23DFiOD}$ and p^{30PUb}, at the *pink-eyed dilution* (*p*) locus on mouse chromosome 7. The two *p* deletions are associated with altered glucose and lipid metabolism and represent a new polygenic mouse model for T2D [11–13]. The model is diet-induced and shows insulin resistance characterized by hyperinsulinemia, hyperglycemia, hyperlipidemia and obesity in association with glucose intolerance. *Atp10c*, a type IV P-type ATPase, a putative aminophospholipid transporter (APLT) linked to the *p-locus*, is identified as a strong candidate for the phenotype. We have shown earlier that for one of the deletions, p^{30PUb}, heterozygous mice with maternal inheritance of *Atp10c* (mutants) fed a high-fat (HF) diet (45% fat−% kcal energy) exhibit a significantly higher body weight, adiposity index and plasma insulin, leptin and triglyceride concentrations compared with the heterozygotes with paternal inheritance of *Atp10c* (controls). The phenotype of mice inheriting the *Atp10c* deletion paternally is similar to that of the wild-type control littermates. Intraperitoneal glucose and insulin tolerance tests (GTT and ITT, respectively) showed altered glucose tolerance and insulin resistance after mice consumed the HF diet for 4 and 8 weeks. Routine gross and histological evaluations of the liver showed severe micro- and macrovesicular lipid deposition within the hepatocytes in the mutant mice. Our data suggest that heterozygous deletion, along with an unusual pattern of maternal inheritance of the chromosomal region containing the single gene *Atp10c*, causes obesity, T2D and nonalcoholic fatty liver disease in these mice [13].

Physical mapping and shotgun sequencing showed *Atp10c/ATP10C* maps to the region between *Gabrb3/GABRB3* and *Ube3a/UBE3A*, on mouse chromosome 7/human chromosome *15q11-q13*, respectively. A part or the whole *Atp10c* gene is deleted in the two *p*-linked deletions, $p^{23DFiOD}$ and p^{30PUb}. *Atp10c* is encoded by 21 exons. All 21 exons including the 5′ and 3′ flanking regions are deleted in the p^{30PUb} heterozygotes. Only the first two exons including the 5′ flanking region are deleted in the $p^{23DFiOD}$ heterozygotes [14,15].

In the present report, we describe results of studies initiated to validate the model via the characterization of the metabolic abnormalities and gene expression changes associated with $p^{23DFiOD}$ mutants and to assess the overall effect of the heterozygous deletion of *Atp10c* on obesity-related phenotypes. We show that after eating the HF diet for 4 weeks, the mutants exhibit no change in their food intake, an increase in their body weights and in the plasma insulin levels ($P>.05$) and are insulin resistant. On the other hand, after 12 weeks, the mutants again exhibit no significant changes in their food intake or their body weights. However, a significant increase in the plasma insulin levels ($P<.05$) and insulin resistance is observed. Insulin-stimulated in vitro glucose uptake in the adipose tissue is significantly impaired after 4 weeks, whereas it is significantly altered in both the adipose tissue and the skeletal muscle after eating the HF diet for 12 weeks. Finally, as demonstrated by both oligo microarray and real-time polymerase chain reaction (PCR) experiments, the expression of insulin signaling pathway genes is dramatically altered in both fat and muscle tissues at both time points. *Atp10c* expression is also affected; it is significantly up-regulated in the adipose tissue and down-regulated in the skeletal muscle at the 12-week stage. Significant changes in biochemical and molecular responses of fat and muscle tissues in *Atp10c* mutants indicate an important role of *ATP10C* in the insulin-mediated clearance of glucose by the peripheral tissues.

2. Materials and methods

2.1. Mice and diet

Female mice carrying the *p* deletion $p^{23DFiOD}$ were generated and maintained as described [11]. From each cross of $p^{23DFiOD}$, a group of p^{x}/p^{l} heterozygotes, which inherited the deletion from their dams (mutants), and a group inheriting the deletion from their sires (controls) were used. All mice were age- and sex-matched. Mice were fed a regular chow diet (Laboratory Rodent Diet, Checkers PMI Nutritional International, Brentwood, MO, USA) until weaning (4–5 weeks old). Thereafter they were weighed and fed a commercial rodent diet (D12451 containing 45% fat (% energy; Research Diets, New Brunswick, NJ, USA) for additional periods of time. All the studies described below were carried out at two specific time points. First was at 8 weeks of age, when the mice have been fed the HF diet for 4 weeks and the second was at 16 weeks of age when they have been fed the HF diet for 12 weeks. The time points were chosen based on the results of our earlier studies [13]. Mice were killed by CO_2 asphyxation. All procedures were in accordance with the Animal Care and Use Committee of the University of Tennessee (protocol number 1309).

2.2. Intraperitoneal insulin tolerance test

Intraperitoneal insulin tolerance test (ITT) was carried out on 8- and 16-week-old conscious mice after eating the HF diet for 4 and 12 weeks, respectively. ITT was carried out as described earlier [13].

2.3. Plasma insulin

Blood was collected and plasma insulin levels were measured using a radioimmunoassay kit with rat insulin as the standard (Linco Research, St. Charles, MI, USA). The experimental protocol was as described by the manufacturer.

2.4. In vitro glucose uptake

Glucose uptake was measured in freshly isolated soleus muscle, white adipose tissue and liver according to standard methods [16–18]. Mice were fasted for 12–16 h and sacrificed; tissues were collected, weighed and minced into small pieces. They were incubated in Krebs-Ringer HEPES buffer (pH 7.4) at 37°C under 5% CO_2 with 95% humidity for 30 min. In the insulin-stimulated measurement, 100 nM of insulin (I-5500 Sigma Aldrich, St. Louis, MO, USA) was used. After 30 min, 1 mCi/ml of the glucose analog, 2-deoxy-D-glucose (^{3}H), was added to the media, and the tissues were further incubated for 1 h. The final total concentration of glucose was maintained as 5 mM. Tissues were then collected, washed in saline, solubilized and the incorporated radioactivity was counted in a scintillation counter (Tri-Carb 2300TR, Perkin Elmer Life and Analytical Services, Boston, MA, USA) using 10 ml of Scintiverse as the scintillation cocktail (Fisher Scientific International, Fairlawn, NJ, USA). Glucose uptake was expressed as disintegrations per minute per gram of tissue (dpm/g). Data is reported as the stimulation/reduction in glucose uptake expressed as the ratio of dpm/g of tissue in presence of insulin to that in the absence of insulin.

2.5. RNA total, cDNA and real time PCR

Total RNA was extracted from the soleus and the adipose tissues using the Trizol method (Invitrogen Carlsbad, CA, USA). RNA was further purified using RNeasy Mini RNA kit (Qiagen, Valencia, CA, USA). RNA concentration was obtained by spectrophotometric analysis. In the second step, RNA was treated with RNase-free DNase I (Promega Madison, WI, USA) and a double-stranded cDNA was synthesized using either the iScript cDNA synthesis kit (Bio-Rad Laboratories, Hercules, CA, USA) or the RETROscript First Strand Synthesis kit for real-time PCR (Ambion, Austin, TX, USA). cDNA was amplified using gene-specific primers by real-time PCR (ABI Prism 7000 Sequence Detection System, Applied Biosystems, Foster City, CA, USA). The primers for real-time PCR were designed using PrimerExpress software (Applied Biosystems) to generate amplicons of approximately 70–100 bp for each gene. The target genes analyzed and the sequence of the respective primers are listed in Table 1A. Mouse *Gapdh* was used as an internal control. PCR reactions were carried out using iTaq SYBR Green Supermix with ROX (Bio-Rad Laboratories). Primer titration and dissociation experiments were performed to ensure specificity of PCR amplification. Each reaction was carried out in a final volume of 25 μl containing 12.5 μl of iTaq SYBR Green Supermix with ROX, 0.5 μM of each gene specific primer and 1 μL of cDNA template from serially diluted concentrations. The standard curve was generated for both the target and the reference genes in each biological sample to ensure the amplification efficiency of about 100%. To generate the standard curve, cDNAs were synthesized with a final concentration of 1 μg/5 μl. This was diluted 1:10 and used as a 1× concentration. The 1× cDNAs were serially diluted to 1:4 and 1:16 generating three template concentrations. Each of the three cDNA templates was used in the PCR reactions. All reactions were carried out in duplicate. The PCR conditions were as follows: 1 cycle of 50°C for 2 min and 95°C for 2 min, followed by 44 cycles of 95°C, 25 s; 52°C, 25 s and 72°C, 1 min. The C_T values were extracted with ABI Prism 7000 SDS Software with auto baseline and appropriate manual C_T. The $2^{-\Delta\Delta C}{}_T$ and standard curve methods were employed to calculate the relative abundance of target gene expression [19].

2.6. Microarray hybridization and data analysis

The mouse whole genome long-oligo set (Operon) were printed on the Powermatrix slides (Full Moon Biosystems, Sunnyvale, CA, USA). One hundred micrograms of total

Table 1
List of genes involved in diabetes, insulin signaling and cardiovascular disease identified in the microarray experiment

Gene ID	Gene name	Gene function	Ratio	S.D.
NM_009097	*Rps6ka1*	Ribosomal protein S6 kinase polypeptide 1	2.49	0.47
NM_009497	*Vamp2*	Vesicle-associated membrane protein 2	2.38	1.12
NM_010271	*Gpd1*	Glycerol-3-phosphate dehydrogenase 1	2.09	0.47
NM_013494	*Cpe*	Carboxypeptidase E	2.07	1.06
NM_011057	*PDGF b*	Platelet-derived growth factor, B polypeptide	2.07	0.21
NM_009204	*Slc2a4*	Solute carrier family 2, member 4	2.05	0.44
NM_010070	*Dok1*	Docking protein 1	2.01	0.20
NM_010548	*IL-10*	Interleukin 10	2.01	0.16
NM_011951	*Mapk14*	Mitogen activated protein kinase 14	1.97	0.39
NM_008404	*Cd18*	Integrin beta 2	1.76	0.28
NM_008401	*Cd11b*	Integrin alpha M	1.67	0.29
NM_016780	*CD61*	Integrin beta 3	1.66	0.12
NM_020009	*Frap1*	FK506-binding protein 12	1.64	0.92
NM_011671	*Ucp2*	Uncoupling protein 2	1.58	0.36
NM_008768	*Orm1*	Orosomucoid 1	0.57	0.29
NM_010284	*Ghr*	Growth hormone receptor	0.57	0.18
NM_007987	*Fas*	Fas (TNF receptor superfamily member)	0.56	0.00

Gene IDs (accession numbers) and their functions are given. Ratio denotes the expression levels of the mutant to the control mice.

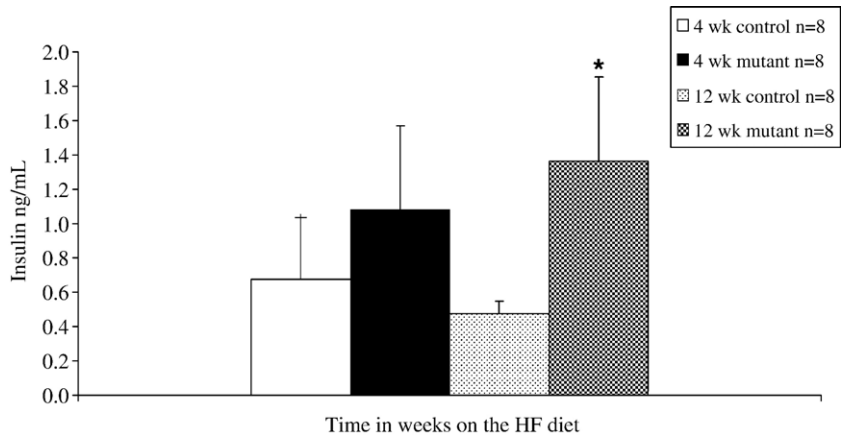

Fig. 1. Plasma insulin concentrations of $p^{23DFiOD}$ mutant and control mice after eating an HF diet for 4 and 12 weeks. Values are shown as mean±S.D. Asterisk indicates $P<.05$ and represents that the mutants have a significantly higher insulin concentration than the control group. For each analysis, n denotes the number of animals used.

RNA for each biological sample was labeled with Superscript III Indirect Labeling Kit (Invitrogen, Carlbad, CA, USA) and hybridized with the mouse whole genome long-oligo microarrays according to the manufacturer's instructions. Reverse labeling experiments were included to eliminate dye-specific bias. For each sample set of mutant versus control, the mutant RNA was first labeled with Cy5 and control with Cy3, and in the reverse experiment, the dyes were swapped. The two labeling reactions and microarray hybridizations were performed in parallel. A total of two biological replicates and two technical replicates for the experiment are included. After hybridization, the microarray slides were washed and scanned in GenePix 4000 scanner, and the image was processed by GenePix Pro software, as described by the manufacturer (Axon Instrument, Union City, CA, USA). The resultant file was analyzed using Microsoft Excel, and only spots with 50% of pixel higher than two times background standard deviation in either color were selected for further data analysis. Bulk normalization was performed for each slide. After normalization, the logarithm (log) 2 transformed ratios for four slides were averaged, and the standard deviations and covariances were calculated. Any gene that has a covariance higher than 50% among the four slides was filtered out. The gene expression ratio between mutant and control RNAs was calculated based on the average log 2-based ratio. The standard deviation of the ratio is estimated from the covariance of log 2-based ratios among the four slides.

2.7. Statistical analysis

Statistical analysis for all biochemical analyses was performed using one-way analysis of variance with Smith's

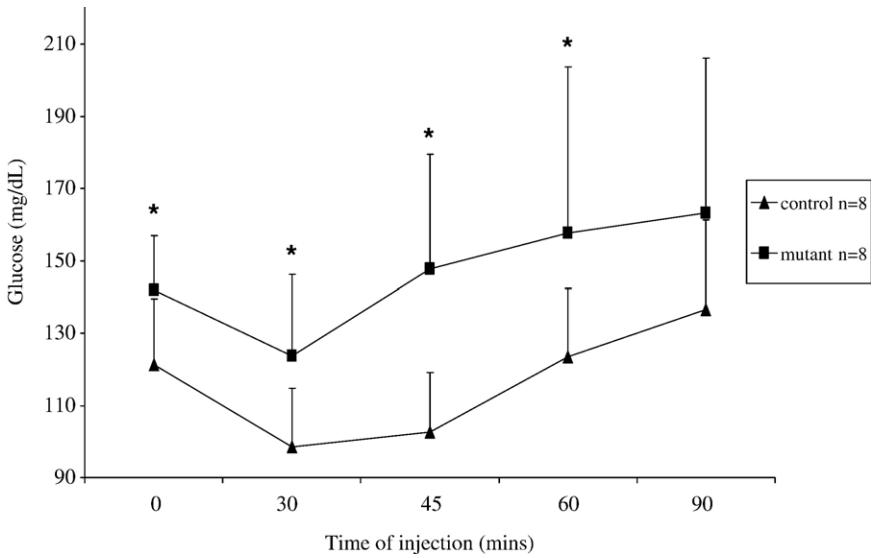

Fig. 2. ITT of $p^{23DFiOD}$ mutant and control mice after eating an HF diet for 12 weeks. Similar trend is observed in mice after eating the HF diet for 4 weeks. Values are shown as mean±S.D. Asterisk indicates $P<.05$ and represents that the mutants are significantly insulin resistant than the control group. For each analysis, n denotes the number of animals used.

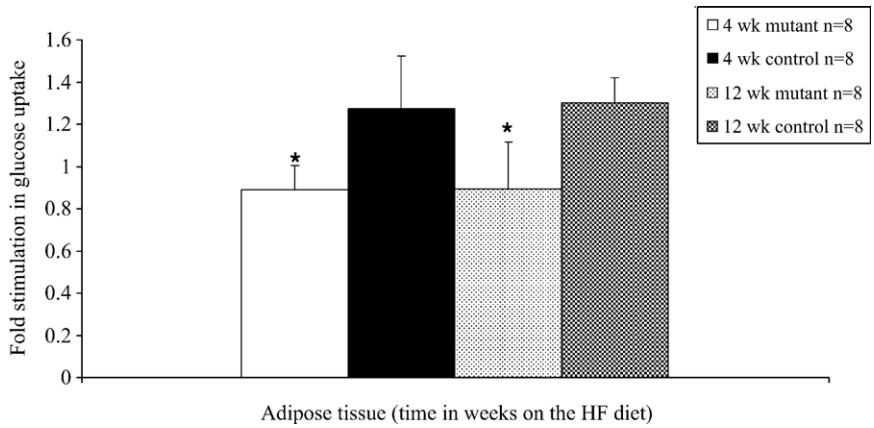

Fig. 3. In vitro glucose uptake in the adipose tissue of $p^{23DFiOD}$ mutant and control mice after eating an HF diet for 4 and 12 weeks. Values are shown as mean±S.D. Asterisk indicates $P<.05$ and represents that the mutants have a significant decrease in fold stimulation of glucose uptake than the control group. For each analysis, n denotes the number of animals used.

Statistical Package Version 2.8 (http://www.economics.pomona.edu/StatSite/SSP.html). $P<.05$ was accepted as statistically significant. Data are presented as the mean±S.D.

Multiple regression model was used for analysis of real-time PCR data [20]. The model estimates the intercept of the multiple standard curves to render P value and standard error for the $\Delta\Delta C_T$, which in turn can be used to determine the ratio for relative gene expression with the $2^{-\Delta\Delta C_T}$ formula. $P<.05$ was accepted as statistically significant.

2.8. Cluster analysis

Cluster analysis was performed by Cluster and Treeview softwares with complete linkage hierarchical clustering methods [21]. The mutant to control ratios are first transformed into log 2 transformed ratios, and then the genes are clustered according to their expression patterns among different tissues and time points. Cluster analyses are performed only for genes and not for different samples.

3. Results

3.1. Effect of HF feeding on plasma insulin concentration and ITT

The mutant mice had 2.8 times significantly higher insulin (1.362 ng/ml, $P<.05$) level than the control mice (0.481 ng/ml) after eating the HF diet for 12 weeks. The insulin levels were only 1.6 times higher in the mutants after eating the same diet for 4 weeks; however, this increase was not significant (Fig. 1). The measurements showed that the mutant mice are hyperinsulinemic after 4 weeks and the degree of hyperinsulinemia increases and becomes significant with time on the HF diet. Data suggests no alteration or defect in insulin secretion. Hence, ITT was performed to determine defect in peripheral signaling. The results are shown in Fig. 2. The mutants exhibited a significantly higher hyperglycemic response to a given dose of insulin after 0, 30, 45 and 60 min than the control age and

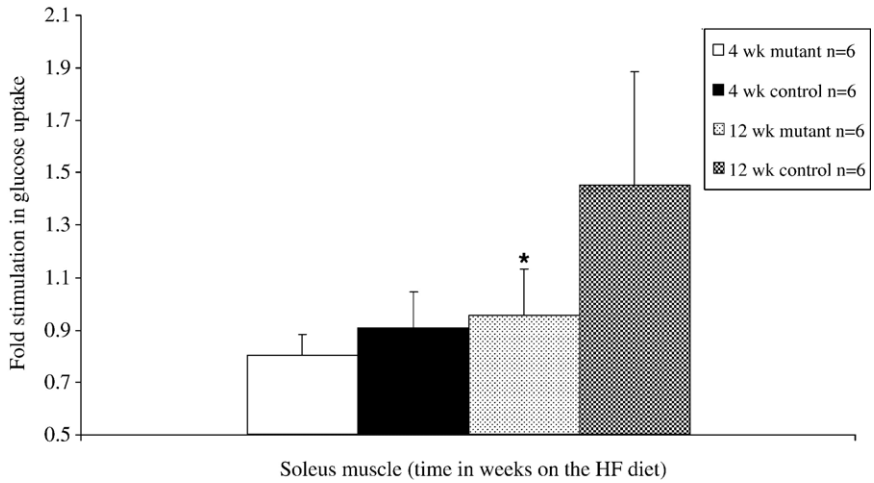

Fig. 4. In vitro glucose uptake in the soleus muscle of $p^{23DFiOD}$ mutant and control mice after eating an HF diet for 4 and 12 weeks. Values are shown as mean±S.D. Asterisk indicates $P<.05$ and represents that the mutants have a significant decrease in fold stimulation of glucose uptake than the control group. For each analysis, n denotes the number of animals used.

Table 2
List of genes selected for real time PCR

Gene	Gene ID	Primers (5′ to 3′)	Reference
Atp10c	NM_009728	CGTGGCTCTGATTTACAACACTTC AAGTAGAACAGAGGGTCACCCAGTA	[14,15]
Dok1	NM_010070	GCAGCAGTTACTGAAAACCAAGCT CCAGGCCTTCAGGTTCATCA	[30]
Glut4	NM_009204	AGCGTAGGTACCAACACTTTCTTGT CCGCCCTTAGTTGGTCAGAAG	[45]
MapK14	NM_011951	AGGGAACGAGAAAACTGCTGTT TATTATCTGACATCCTATGGCATACCA	[46]
Vamp2	NM_009497	CAAAACAGAATCCCCCTAATTCC AAGTTTTCAGTCGAACCTCTAGCAA	[47]
Gapdh	NM_017008	TGCACCACCAACTGCTTAG GATGCAGGGATGATGTTC	[48]

Gene names and their IDs (accession numbers) are given. The sequence listed in the first line is the forward primer and the second line represents the sequence of the reverse primer for each gene.

sex-matched mice after eating the HF diet for both 4 and 12 weeks ($P<.05$).

3.2. Effect of HF feeding on glucose uptake

Since glucose uptake is the key step in maintaining glucose homeostasis in the peripheral tissues, we next investigated the process of in vitro glucose uptake in skeletal muscle, adipose tissue and liver. Glucose uptake was measured in the adipose tissue and the soleus muscle in the basal (without insulin) and in the stimulated (with 100 nM insulin) states. Since glucose disposal in the liver is not insulin-stimulated, only the basal levels were measured. Results are as shown in Figs. 3 and 4. Adipose tissue in the mutant group exhibited significant glucose uptake impairment after eating the HF diet for both 4 and 12 weeks ($P<.005$); however, the soleus muscle showed a significant impairment only after 12 weeks ($P<.05$). There was a 30% decrease in insulin-stimulated response in the adipose tissue at both time points; however, a decrease of 35% in the soleus muscle was achieved only after eating the HF diet for 12 weeks. In the liver, there is a 4% reduction in glucose uptake in the mutants after 4 weeks, whereas there is 18.5% decrease after 12 weeks. These values are not statistically significant but suggest a trend and that significance will be attained as the disease progresses.

3.3. Identification and characterization of diabetes and obesity genes after HF feeding

To characterize the metabolic defect described above at the molecular level, gene expression profiling was undertaken. Microarray analysis was carried out using total RNA isolated from the adipose tissue from the mutant and the control mice after eating the HF diet for 12 weeks. The mouse microarrays were produced from the Operon mouse array ready-oligo set with 31,769 probes representing 24,878 genes and 32,829 transcripts. Two hundred thirty genes (0.69%) showed a significantly higher expression in mutant adipose tissue, and 50 genes (0.15%) were significantly down-regulated in mutant adipose tissue. Table 1 lists the diabetes, insulin signaling and genes involved in cardiovascular disease that were differentially regulated at this stage. Out of these, a set of genes involved in insulin-stimulated glucose uptake was selected for further quantitation by real-time PCR (Table 2). *Atp10c* was also included in the analysis. Mouse *Gapdh* was used as an internal control. The results indicate a close agreement between the microarray data with that obtained from the real-time PCR analyses.

As described below, mouse *Glut 4, Vamp2, Dok1* and *Mapk14* selected for real-time PCR are all known to be involved in the GLUT4-mediated glucose uptake in the

Table 3
Real-time PCR of five genes with the adipose tissue and the soleus muscle RNAs derived from $p^{23DFiOD}$ mutant and control mice after eating an HF diet for 4 weeks

Tissue type	Gene	$\Delta\Delta C_T$	S.D.	*P* value	Mutant/control
Adipose	*Atp10c*	−0.2993	0.1897	.1458	0.812647
Adipose	*Dok14*	0.4557	0.1304	.005*	1.371448
Adipose	*Glut4*	−1.0882	0.1599	<.0001*	0.470348
Adipose	*MapK14*	−0.439	0.1429	.0097*	0.737646
Adipose	*Vamp2*	−0.1105	0.1519	.4815	0.926267
Muscle	*Atp10c*	−0.5986	0.1397	.0016*	0.660394
Muscle	*Dok1*	−0.1646	0.1479	.2982	0.892176
Muscle	*Glut4*	0.8687	0.1005	<.0001*	1.826017
Muscle	*MapK14*	1.2515	0.0824	<.001*	2.380888
Muscle	*Vamp2*	1.1943	0.1185	<.001*	2.288338

Mutant/control is the ratio of gene expression of the mutant to the control RNA. Asterisk indicates significant difference in mutant versus the control group ($P<.05$).

Table 4
Real-time PCR analyses of five genes with the adipose tissue and the soleus muscle RNAs derived from $p^{23DFiOD}$ mutant and control mice after eating an HF diet for 12 weeks

Tissue type	Gene	$\Delta\Delta C_T$	S.D.	P value	Mutant/control
Adipose	*Atp10c*	1.4145	0.3093	.0006*	2.665673
Adipose	*Dok14*	0.9025	0.2615	.0054*	1.869302
Adipose	*Glut4*	2.24	0.2098	<.0001*	4.723971
Adipose	*MapK14*	1.2515	0.08239	<.0001*	2.380888
Adipose	*Vamp2*	0.7665	0.2211	.0047*	1.701138
Muscle	*Atp10c*	−7.7792	0.6887	<.0001*	0.004552
Muscle	*Dok1*	−2.962	0.5504	.0013*	0.128336
Muscle	*Glut4*	−0.4533	0.3666	.0001*	0.266406
Muscle	*MapK14*	−1.8887	0.5142	.0009*	0.27005
Muscle	*Vamp2*	0.8491	0.5575	.0426*	1.801377

Mutant/Control is the ratio of gene expression of the mutant to the control RNA. Asterisk indicates significant difference in mutant versus the control group (P <.05).

peripheral tissues. As illustrated in Tables 3 and 4, the changes are significant in both the adipose tissue and the soleus muscle at both time points. Dramatic changes are observed in *Atp10c* and *Glut4* expression patterns. After eating the HF diet for 4 weeks, the mutants show 82% increase in *Glut4* expression in the soleus muscle, whereas there is a 50% decrease in the adipose tissue. The changes are statistically significant. There is a 66% significant decrease in the *Atp10c* expression only in the soleus muscle, no significant change is observed in the adipose tissue.

On the other hand, in the mutant mice, after 12 weeks of eating the HF diet, all the genes are significantly up-regulated in the adipose tissue, whereas they are down-regulated in the soleus muscle. Importantly, there is about a 100% decrease in *Atp10c* expression in the muscle compared to a 26% decrease in *Glut4* expression. Correspondingly, there are a 3% and a 5% increase in both the *Atp10c* and *Glut4* expressions, respectively, in the adipose tissue. The fold difference in expression between the mutant and control groups is greater after eating the HF diet for 12 weeks compared to that after 4 weeks. This is confirmed by the Cluster analysis shown in Fig. 5.

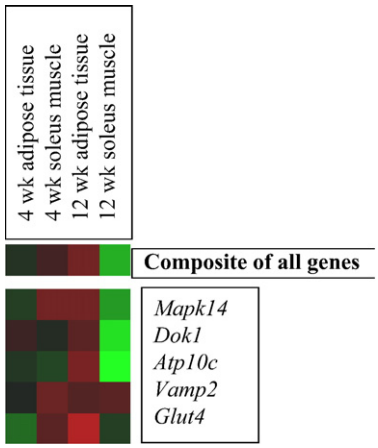

Fig. 5. Cluster analysis of five target genes expressed in the adipose tissue and the soleus muscle of $p^{23DFiOD}$ mutant and control mice after eating an HF diet for 4 and 12 weeks. The color represents the expression level of the target genes. Gene expression is denoted as the ratio of the mutant to the control group. The red color represents the expression ratio of greater than 1, and the green color represents the ratio of less than 1. The levels of gene expression are directly related to the intensity of the color — higher gene expression is shown with a brighter intensity.

4. Discussion

We have reported earlier that a type IV P-type ATPase, *Atp10c*, may be involved in glucose and lipid metabolism in mice [12,13]. The current study was initiated to further validate our model via the identification of the metabolic abnormalities associated with the heterozygous deletion of mouse *Atp10c* and the genes involved in adipose tissue and skeletal muscle physiology affected by this deletion. Supporting our earlier observation in p^{30PUb} heterozygotes, we have clearly shown here that the insulin resistance of $p^{23DFiOD}$ heterozygotes is due to the maternal inheritance of *Atp10c* and that the severity of the disease progresses with time on the HF diet [13].

Comparison of the biochemical and molecular data between the mutant and their control littermates shows that the mutants exhibit significant insulin resistance after eating an HF diet for 4 and 12 weeks, and the phenotype is primarily due to a defect in insulin signaling and not insulin secretion. Glucose uptake is significantly impaired in the adipose tissue in the 4-week state, whereas a defect is observed in both the adipose tissue and the soleus muscle at the 12-week time. Data support our earlier hypothesis that the phenotype is diet-induced and that insulin resistance precedes obesity. Insulin resistance primarily affects the adipose tissue and the skeletal muscle, and the effect in the liver is secondary [13]. Real-time PCR shows significant changes in the expression of genes, specifically *Glut4*, the key player involved in insulin-mediated glucose uptake at the two time points. The expression of *Atp10c* is also significantly altered in the adipose tissue and the soleus muscle in the two states. The changes in expression are greater after 12 weeks. The most striking result is the loss of *Atp10c* expression in the mutants, specifically in the soleus muscle. This is the first report wherein we have observed significant changes in *Atp10c* expression of the maternal allele compared to that of the paternal allele.

Diabetes is a disorder of glucose metabolism caused by a decrease in the clearance of glucose from the blood stream. Non-insulin dependent or T2D is characterized by hyperinsulinemia and peripheral insulin resistance. Insulin resistance is due to a defect in the peripheral tissues — adipose tissue and the skeletal muscle [1–4]. Adipose tissue accounts for only 5–10% of insulin-mediated glucose uptake, whereas the majority of glucose is disposed by the skeletal muscle. Hence, skeletal muscle is considered as an important target for glucose uptake; however, recent studies in transgenic animal models clearly show an important role of the adipose tissue in glucose homeostasis as well [22–27]. Thus, both the adipose tissue and the skeletal muscle are the foci of interest in the pathogenesis of insulin resistance.

Insulin-induced glucose uptake into muscle and adipose tissue is a key factor in the maintenance of glucose homeostasis. In all types of obesity and T2D, the major abnormality lies in the glucose uptake system. It involves a series of intracellular signaling cascades culminating in glucose disposal and metabolism [22–27]. Transgenic mouse models clearly reveal that the intracellular signaling cascades upstream to phosphatidylinositol-3-kinase (P13 kinase) are much more clearly understood, whereas the metabolic events leading to the translocation of GLUT4 and downstream to P13 kinase are difficult to interpret. The mechanism by which the activation of P13 kinase results in GLUT4 translocation remains unclear. Literature shows that in insulin-resistant states (obesity and T2D) in humans and rodents, GLUT4 expression is down-regulated in the adipose tissue, whereas in the skeletal muscle, it is due to an altered translocation of intracellular GLUT4, presumably due to defects in GLUT4 trafficking and/or targeting. Besides changes in GLUT4, there are other mechanisms affecting insulin resistance and other insulin signaling molecules in morbidly obese and insulin-resistant humans [25–27]. Understanding the mechanisms involved in insulin action in a cell may be useful to identify new targets in insulin resistance.

Our in vitro glucose uptake results show that all three target tissues — adipose tissue, skeletal muscle and liver are affected in the mutants. There is clearly a difference in the severity and the time at which each tissue is affected. Adipose tissue is the first target tissue affected, and then the disease spreads to the skeletal muscle and, finally, the liver. A decreased glucose uptake in the adipose tissue is presumably the initiating event leading to a complex phenotype in the mutants, which ultimately affects skeletal muscle and liver. Quantitation of gene expression shows that in the adipose tissue, the levels of *Glut4, Vamp2, Mapk, Dok1* and *Atp10c* expression were significantly up-regulated in the mutants after 12 weeks of HF feeding. These data taken together with the insulin-stimulated glucose uptake suggest that in the adipose tissue, the insulin resistance is presumably due to a decrease/lack of the protein expression and/or a defective function of the protein and not due to a decrease in the mRNAs. On the other hand, in the soleus muscle, all the genes were significantly down-regulated, suggesting a decrease at the mRNA level, which may then get translated to an altered protein expression subsequently leading to a change in its function. Taken together, the target genes identified by microarray analysis, in conjunction with *Atp10c*, presumably affect GLUT4 translocation in both the target tissues.

Glucose uptake due to GLUT4 exocytosis involves three major steps — insulin signaling to GLUT4 vesicles, trafficking of GLUT4 vesicles to the plasma membrane and finally docking and fusion of GLUT4 vesicles with the plasma membrane. The genes analyzed in the current study play major roles in at least one of the three steps. Of all the genes selected, GLUT4 has been extensively studied. GLUT4 is the predominant glucose transporter isoform expressed in the adipose tissue and skeletal muscle and catalyses the rate-limiting step for glucose uptake and metabolism [27]. VAMP2 is a vesicle-associated protein 2 associated with GLUT4-containing vesicles in adipocytes and skeletal muscle. VAMP2 is a member of the soluble *N*-ethylmaleimide-sensitive factor attachment protein receptors (SNARE) complex of proteins. VAMP2 interacts with SNAP23 and syntaxin 4 initiating GLUT4-vesicle exocytosis [28,29]. GLUT4 vesicle exocytosis resembles that of the synaptic vesicles. SNARE proteins are suggested to play important role in the docking and fusion of the GLUT4-containing vesicles to the plasma membrane. It has been suggested that the SNARE proteins found in adipocytes might be involved in the molecular regulation of glucose transport in the adipose tissue. Thus, any change in VAMP2 expression can alter GLUT4 translocation. Even though their biological roles in neurosecretory vesicle docking and fusion events have been extensively characterized; the exact mechanism by which insulin might regulate the SNARE components remains unknown. DOK1 is a docking protein 1 suggested to be a substrate for tyrosine kinases. It belongs to a newly identified class of adapter proteins. It has been suggested that DOK1 interacts with P13 kinase and, hence, is involved in insulin signaling [30–32]. Its biological roles are not yet clearly characterized, but based on the information available, it is reasonable to suggest that its interaction with P13 kinase might indirectly lead to changes in intracellular signaling cascades downstream of P13 kinase, resulting in an altered glucose uptake. MAP kinase signaling pathways also play an important role in insulin stimulation of glucose uptake [33,34]. Hence, it is not surprising that the expression of MAPK14, a member of this family of proteins, is affected.

Atp10c is a type IV P-type ATPase, a putative APLT. P-type ATPases are the most extensively studied membrane transporters [35,36]. Two well-recognized subfamilies have been described, and recently, a third subfamily proposed to be transbilayer amphipath transporters has been identified [37–39]. The exact function of the members of the third type is still not known. APLTs are proposed to translocate phosphatidylserine (PS) and/or phosphatidylethanolamine

(PE) from one leaflet of the bilayer membrane to the other and, thus, play a role in maintaining the fluidity and the asymmetry of the lipid bilayer [40,41]. Cloning and comparison of a bovine and a murine class II ATPase purified from chromaffin granules with the previously identified yeast class II gene, DRS2, suggested that aminophospholipid translocation could be a general function of members of this subfamily [42–44]. Recently, Natarajan et al. [44] have provided compelling evidence to show that the *Drs2* gene is indeed an APLT. The authors have demonstrated the translocation of the flip-labeled phospholipid derivatives of PE and PS. This is the first report demonstrating the role of APLTs in protein trafficking across the plasma membrane. In the last 5 years, five genes from this subfamily have been cloned and characterized, and their putative functions have been linked to a few biological disorders [44]. Although detailed and conclusive experiments to study the mechanisms to confirm the role of phospholipid translocases in regulating various cellular functions (specifically insulin action) are not available, the importance of type IV P-type ATPases in human research is becoming patently clear.

The current experiments clearly demonstrate that heterozygous mutants for *Atp10c* are hyperinsulinemic, insulin resistant and have an altered insulin-stimulated response in peripheral tissues. Adipose tissue and the skeletal muscle are the targets, and GLUT4-mediated glucose uptake is the specific metabolic pathway associated with *Atp10c* deletion. Results presented here strengthen our hypothesis that loss of ATP10C function by maternal deletion can upset the normal membrane milieu and perturb glucose metabolism. It is conceivable that *Atp10c* along with other genes (*Glut4, Vamp2, Dok1 and Mapk14)* and their cognate factors involved in insulin signaling affect the normal translocation of GLUT4. The exact mechanism underlying the phenotype now needs to be investigated.

In view of the data presented here and the literature discussed, we have a unique opportunity in this model to dissect this metabolic pathway to gain a better understanding of the molecular mechanisms of GLUT4 sequestration and trafficking. Specific targeted experiments to generate adipose tissue and skeletal muscle-specific transgenics, assess protein expression of target genes and carry out translocation assays can now be initiated.

Acknowledgments

We thank Dr. Nicholas Frank, Dr. Patty Titoff and Dr. Todd Graham for their valuable comments on the manuscript.

References

[1] Kahn BB, Flier JS. Obesity and insulin resistance. J Clin Invest 2000;106(4):473–81.
[2] Rao G. Insulin resistance syndrome. Am Fam Physician 2001;63(6):1159–63.
[3] Saltiel AR, Kahn R. Insulin signaling and the regulation of glucose and lipid metabolism. Nature 2001;414:799–806.
[4] Vollenweider P. Insulin resistant states and insulin signaling. Clin Chem Lab Med 2003;41(9):1107–19.
[5] Mora S, Pessin JE. An adipocentric view of signaling and intracellular trafficking. Diabetes Metab Res Rev 2002;18:345–56.
[6] Bryant NJ, Govers R, James DE. Regulated transport of the glucose transporter GLUT4. Nat Rev Mol Cell Biol 2002;3(4):267–77.
[7] Minokoshi Y, Kahn CR, Kahn BB. Tissue-specific ablation of the GLUT4 glucose transporter or the insulin receptor challenges assumptions about insulin action and glucose homeostasis. J Biol Chem 2003;278(36):33609–12.
[8] West DB, Ma Y, Truett AA, York B. Identification of genes involved in animal models of obesity. In: Lockwood DH, Heffner TG, editors. Obesity: pathology and therapy handbook of pharmacology. New York: Springer Verlag; 2000. p. 427–59.
[9] Rees DA, Alcolado JC. Animal models of diabetes mellitus. Diabet Med 2005;22:359–70.
[10] Sima AAF, Shafir E. Animal models of diabetes: a primer. Amsterdam: Harwood Academic Publishers; 2000.
[11] Dhar MS, Johnson DK. A microsatellite map of the *pink-eyed dilution (p)* deletion complex in mouse chromosome 7. Mamm Genome 1997;8:143–5.
[12] Dhar M, Webb LS, Smith L, Hauser LH, Johnson D, West DB. A novel ATPase on mouse chromosome 7 is a candidate gene for increased body fat. Physiol Genomics 2000;4:93–100.
[13] Dhar MS, Sommardahl CS, Kirkland T, Nelson S, Donnell R, Johnson DK, et al. Mice heterozygous for *Atp10c*, a putative amphipath, represent a novel model of obesity and type 2 diabetes. J Nutr 2004;134(4):799–805.
[14] Dhar M, Hauser L, Johnson DK. Genomic structure of a murine aminophospholipid translocase mapping to a quantitative trait locus influencing body fat and associated with type 2 diabetes phenotype. Obes Res 2002;10(7):695–702.
[15] Dhar MS, Hauser LJ, Nicholls RD, Johnson DK. Physical mapping of the *pink-eyed dilution* complex in mouse chromosome 7 shows that *Atp10c* is the only transcript between *Gabrb3* and *Ube3a*. DNA Seq 2004;15(4):306–9.
[16] Cuendet GS, Loten EG, Jeanrenaud B, Renold AE. Decreased basal, noninsulin-stimulated glucose uptake and metabolism by skeletal soleus muscle isolated from obese-hyperglycemic (ob/ob) mice. J Clin Invest 1976;58:1078–88.
[17] Carey AL, Lamont B, Andrikopoulos S, Koukoulas I, Proietto J, Febbraio MA. Interleukin-6 gene expression is increased in insulin-resistant rat skeletal muscle following insulin stimulation. Biochem Biophys Res Commun 2003;302(4):837–40.
[18] Zisman A, Peroni OD, Abel ED, Michael MD, Mauvais-Jarvis F, Lowell BB, et al. Targeted disruption of the glucose transporter 4 selectively in muscle causes insulin resistance and glucose intolerance. Nat Med 2000;6(8):924–8.
[19] Livak KJ, Schmittgen TD. Analysis of relative gene expression data using real-time quantitative PCR and the 2(−Delta Delta C(T)) method. Methods 2001;25(4):402–8.
[20] Yuan JS, Stewart Jr CN. Real-time PCR statistics. PCR Encyclopedia 2005;1:101127–49.
[21] Eisen MB, Spellman PT, Brown PO, Botstein D. Cluster analysis and display of genome-wide expression patterns. Proc Natl Acad Sci U S A 1998;95(25):14863–8.
[22] Katz EB, Burcelin R, Tsao T-S, Stenbit AE, Charron MJ. The metabolic consequences of altered glucose transporter expression in transgenic mice. J Mol Med 1996;74:639–52.
[23] Watson RT, Kanzaki M, Pessin JE. Regulated membrane trafficking of the insulin responsive glucose transporter 4 in adipocytes. Endocr Rev 2004;25(2):177–204.
[24] Shulman GI. Cellular mechanisms of insulin resistance. J Clin Invest 2000;106(2):171–6.

[25] Watson RT, Pessin JF. Intracellular organization of insulin signaling and GLUT4 translocation. Recent Prog Horm Res 2001;56: 175–93.
[26] Shepherd PR, Kahn BB. Glucose transporters and insulin action: implications for insulin resistance and diabetes mellitus. N Engl J Med 1999;341(4):248–57.
[27] Wallberg-Henriksson H, Zierath JR. GLUT4: a key player regulating glucose homeostasis? Insights from transgenic and knockout mice. Mol Membr Biol 2001;18:205–11.
[28] Cheatham B. GLUT4 and company: SNAREing roles in insulin-regulated glucose uptake. Trends Endocrinol Metab 2000;11(9): 356–61.
[29] Kawanishi M, Tamori Y, Okazawa H, Araki S, Shinoda H, Kasuga M. Role of SNAP23 in insulin-induced translocation of GLUT4 in 3T3-L1 adipocytes. Mediation of complex formation between syntaxin4 and VAMP2. J Biol Chem 2000;275(11):8240–7.
[30] Shinohara H, Inoue A, Toyama-Sorimachi N, Nagai Y, Yasuda T, Suzuki H, et al. Dok-1 and Dok-2 are negative regulators of lipopolysaccharide-induced signaling. J Exp Med 2005;201(3):333–9.
[31] Liang X, Wisniewski D, Strife A, Shivakrupa S, Clarkson B, Resh MD. Phosphatidylinositol 3-kinase and Src family kinases are required for phosphorylation and membrane recruitment of Dok-1 in c-Kit signaling. J Biol Chem 2002;277(16):13732–8.
[32] White MF. The IRS-signalling system: a network of docking proteins that mediate insulin action. Mol Cell Biochem 1998; 182(1-2):3–11.
[33] Zhao M, Schmitz AA, Qin Y, Di Cristofano A, Pandolfi PP, Van Aelst L. Phosphoinositide 3-kinase-dependent membrane recruitment of p62(dok) is essential for its negative effect on mitogen-activated protein (MAP) kinase activation. J Exp Med 2001;194(3): 265–74.
[34] Pandya N, Santani D, Jain S. Role of mitogen-activated protein (MAP) kinases in cardiovascular diseases. Cardiovasc Drug Rev 2005;23(3):247–54.
[35] Maeda M, Hamano K, Hirano Y, Suzuki M, Takahashi E, Terada T, et al. Structures of P-type transporting ATPases and chromosomal locations of their genes. Cell Struct Funct 1998;23(6):315–23.
[36] Moller JV, Juul B, le Maire M. Structural organization, ion transport, and energy transduction of P-type ATPases. Biochim Biophys Acta 1996;1286:1–51.
[37] Halleck MS, Pradhan D, Blackman C, Berkes C, Williamson P, Schlegel RA. Multiple members of a third subfamily of P-type ATPases identified by genomic sequences and ESTs. Genome Res 1998;8:354–61.
[38] Halleck MS, Lawler Jr JF, Blackshaw S, Gao L, Nagarajan P, Hacker C, et al. Differential expression of putative transbilayer amphipath transporters. Physiol Genomics 1999;1:139–50.
[39] Tang X, Halleck MS, Schlegel RA, Williamson PL. A subfamily of P-type ATPases with aminophospholipid transporting activity. Science 1996;272:1495–7.
[40] Williamson PL, Schlegel RA. Transbilayer phospholipid movement and clearance of apoptotic cells. Biochim Biophys Acta 2002;1585: 53–63.
[41] Graham TR. Flippases and vesicle-mediated protein transport. Trends Cell Biol 2004;14(2):670–7.
[42] Ding JT, Wu Z, Crider BP, Ma YM, Li XJ, Slaughter C, et al. Identification and functional expression of four isoforms of ATPase II, the putative aminophospholipid translocase — effect of isoform variation on the ATPase activity and phospholipid specificity. J Biol Chem 2000;275:23378–86.
[43] Bull LN, van Ejik MJ, Pawlikowska L, DeYoung JA, Juijn JA, et al. A gene encoding a P-type ATPase mutated in two forms of hereditary cholestasis. Nat Genet 1998;18:219–24.
[44] Natarajan P, Wang J, Hua Z, Graham TR. Drs2-coupled aminophospholipid translocase activity in yeast Golgi membranes and relationship to in vivo function. Proc Natl Acad Sci U S A 2004; 101(29):10614–9.
[45] Ewart MA, Clarke M, Kane S, Chamberlain LH, Gould GW. Evidence for a role of the exocyst in insulin-stimulated trafficking in 3T3-L1 adipocytes. J Biol Chem 2005;280(5):3812–6.
[46] Huang C, Thirone AC, Huang X, Klip A. Differential contribution of insulin receptor substrates 1 versus 2 to insulin signaling and glucose uptake in l6 myotubes. J Biol Chem 2005;280(19):19426–35.
[47] Carvalho E, Schellhorn SE, Zabolotny JM, Martin S, Tozzo E, Peroni OD, et al. GLUT4 overexpression or deficiency in adipocytes of transgenic mice alters the composition of GLUT4 vesicles and the subcellular localization of GLUT4 and insulin-responsive aminopeptidase. J Biol Chem 2004;279(20):21598–605.
[48] Schmittgen TD, Zakrajsek BA. Effect of experimental treatment on housekeeping gene expression: validation by real time, quantitative RT-PCR. J Biochem Biophys Methods 2000;46:69–81.